

**2020 PIL Geochemistry and SWIR Analysis**

Finlay Minerals Ltd.

2020-12-16

Darcy Vis B.Sc., P.Geo.

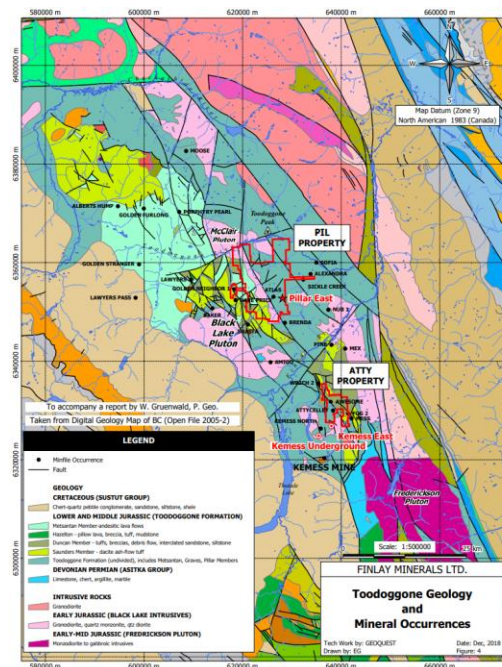
Tripoint Geological Services Ltd.

## 1 SUMMARY

A surface sampling and mapping campaign was completed on the PIL Property by Tripoint Geological Services Ltd. between July 24, 2020 – August 13, 2020. The purpose of the campaign was to further our understanding of the geology, as well as attempt to determine the source and nature of the mineralization and surface anomalies on the property. The rock samples obtained from the property were sent for Assay at ALS Geochemistry using a 4-acid trace ICP-AES/ICP-MS method (ME-MS61) in order to fingerprint composition, alteration, and mineralization of various rock units over the property. The assay data was processed and plotted into various graphs and diagrams in attempt to determine rock composition, alteration, and magma fertility. A Terraspec Halo ASD device was used to collect SWIR/NIR data, which was processed using the CSIRO TSG spectral library. The SWIR/NIR data was then compared to the Geochemistry, and alteration assemblages were separated and determined with the help of both the field notes and rock hand samples.

## 2 REGIONAL GEOLOGY

The PIL Property sits within the Toodoggone Region, a roughly 90km by 15km wide northwesterly trending belt of volcanic and intrusive rocks. The regional lithologies include volcanics and several intrusive bodies ranging from Early Jurassic to Early Permian in age. The region is dominated by subaerial Jurassic age Hazelton Group volcanoclastics, tuffs, and andesite flows. This is underlain by the Triassic age Takla Group volcanic basalts and andesites. The Takla group has been intruded by a series of intrusives including Granodiorites, Monzodiorites, Gabbros, and the Early Jurassic Black Lake Intrusives (Gruenwald 2018).



### **3 ASSAY METHODS**

---

Rock samples collected in 2020 were sent to ALS Geochemistry for preparation and assaying. The prep work was completed in Kamloops, and the assays were completed in North Vancouver. The following methods were used:

#### **PREP-31**

The sample was logged, weighed, dried, and finely crushed to better than 70% passing a 2mm screen. The sample was then split, then pulverized to 85% passing a 75 micron screen.

#### **ME-MS61**

The assays were completed by digesting the sample with a four-acid mixture composed of perchloric, nitric, and hydrofluoric acids. The residue is leached using dilute hydrochloric acid and diluted to volume. The sample is then run through ICP-AES (atomic emission spectroscopy), then ICP-MS (Mass Spectroscopy). This method quantitatively dissolves nearly all minerals except for corundum, kyanite, garnet, staurolite, topaz, and tourmaline. Potassium may also be low due to the formation of insoluble perchlorate. Al and Ca might be low if the sample was not taken to incipient dryness, and insoluble fluoride complexes were created.

#### **Au-AA23**

All samples were run through a 30g Fire Assay Fusion, with AAS finish.

## 4 TERRASPEC SWIR

A Terraspec Halo ASD Device was used to collect Short Wave and Near Infrared spectra, which was then processed using CSRIO spectral software “The Spectral Geologist”. Chip samples collected over the PIL Property were scanned using the ASD device and spectral information was collected. The spectra were then compared to the TSG spectral library to provide mineral picks, which was reviewed by the author for validity.

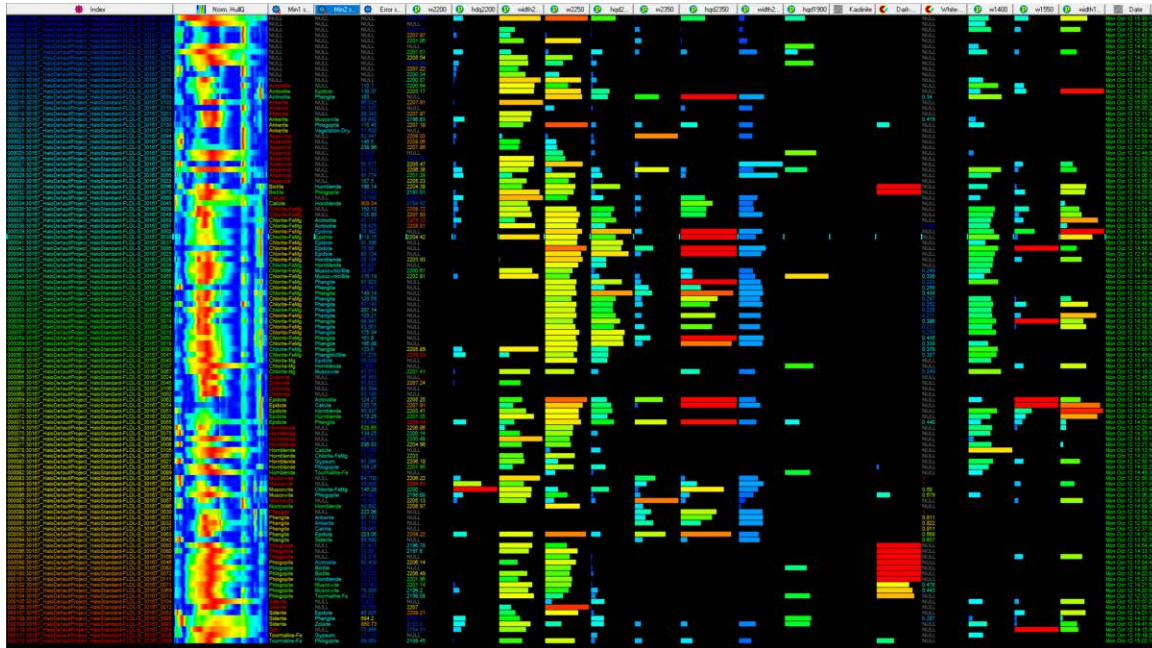


Figure 1. Spectral Geologist Software Output.

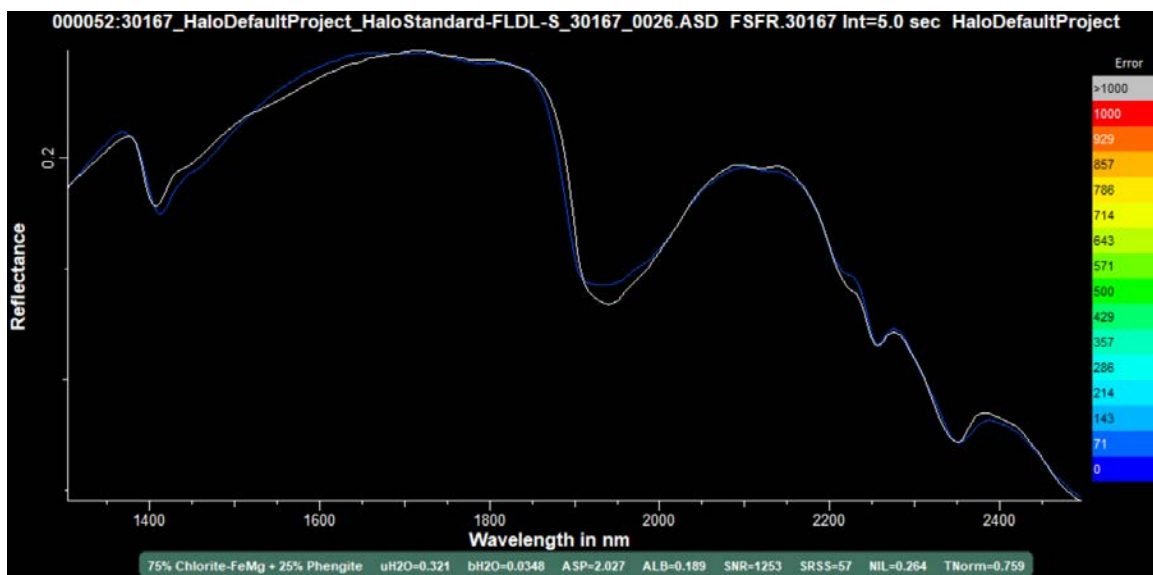


Figure 2. Reflectance vs Light Wavelength Line. White Line is measured, blue line is reference (75% Chlorite, 25% Phengite)

## 5 GEOCHEMISTRY ANALYSIS

The elements were pulled from the 2020 ALS Lab Certificates and were converted to numeric values. Anything below detection limit was changed to a negative number, anything above detection limits had a .999 added to the number. The lithology and sample locations were recorded from the sample notes. Caution should always be used when interpreting trace geochemistry as no one plot will provide sufficient evidence to make any claims. However, by using numerous plots, and confirming with the geology and other methods (Terraspec), we can build confidence in the interpretation.

### 5.1 CALIBRATION CHECKING

To check the validity of the assay samples we first test the precision. Certain elements that are highly correlated can be plotted to see the precision of the assays, these include La and Ce, Hf and Zr, and Ta and Nb. The 2020 Assay Samples show good precision.

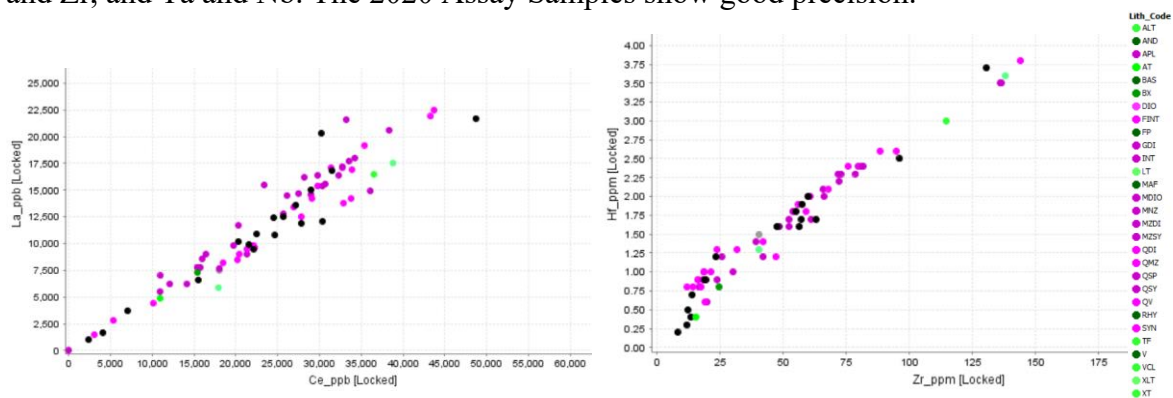


Figure 3. La vs Ce, Hf vs Zr shows precision of assays.

### Aluminum Test

It is highly unlikely for samples to plot above the albite-orthoclase tie line. Plotting K/Al vs Na/Al we can see that they took each sample to incipient dryness and no insoluble flouride complexes were created. The Aluminum values can be trusted.

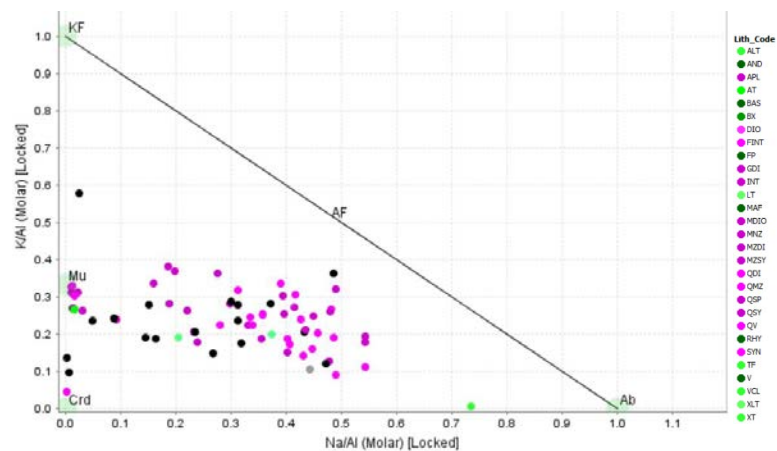


Figure 4. Feldspar GER Diagram

## Magmatic Differentiation

Sc is correlated with silicate-hosted component of Fe, and is hosted in Fe-Mg minerals such as pyroxene and amphibole. It also is immobile in most weathering and hydrothermal environments (Williams-Jones and Vasyukova 2018). This makes it a perfect element to compare other values to as it isn't affected by alteration.

First-row transition metals including Sc, V, Mn, Fe, Co, Ni, Cu, and Zn have similar chemical properties and will plot in a linear relationship with Sc, which decreases with magmatic differentiation. A departure from the linear trend is indication of fractionation of opaque oxide minerals, sulphide saturation in melts, or leaching of metals during hydrothermal alteration. Mn and Zn are the most soluble of the transition metals and can highlight areas of metal leaching caused by hydrothermal alteration or metal enrichment (Wilkinson et al 2015).

In the plots below we can see depletion of Sc with increasing Mn and Zn, showing either metal leaching by hydrothermal alteration or metal enrichment.

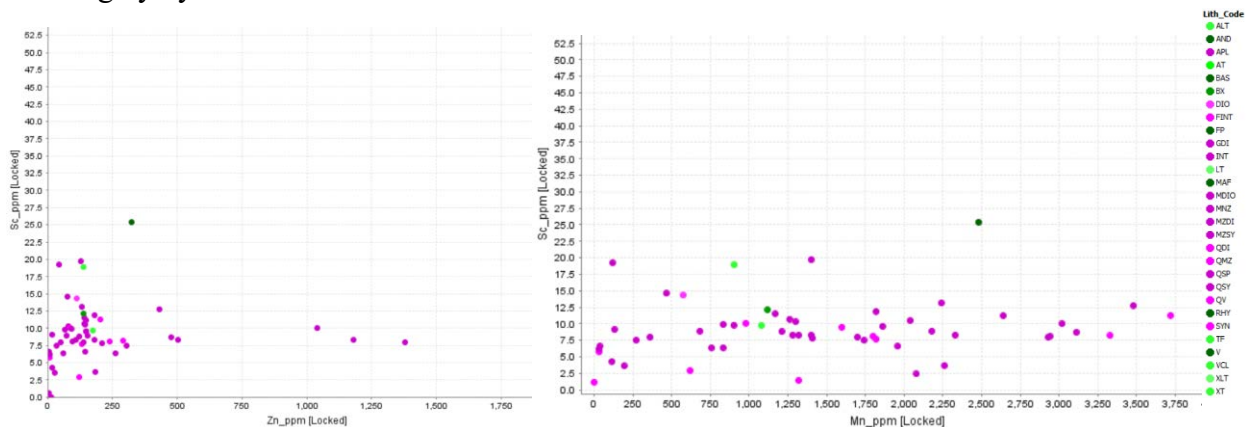


Figure 5. Sc Vs Mn,Zn showing either hydrothermal alteration or metal leaching.

## 5.2 ROCK COMPOSITIONS

Geochemistry can be used to identify the composition of rocks that are similar, but doesn't distinguish between rock types. A single magmatic event can produce intrusive, extrusive, volcanoclastic and epiclastic rocks with the same composition but different textures and rock types. Plotting Sc vs Th, Ti, Nb, and V can show the different magmatic origins. High Sc to Low Sc shows compositional ranges from mafic to felsic (High Sc = Mafic, Low Sc = Felsic).

The magma chamber was maturing from mafic to felsic during the intrusion events, however more data points are needed to separate possible clusters into separate magmatic events, but we can see there was at least two (blue circle, orange circle).

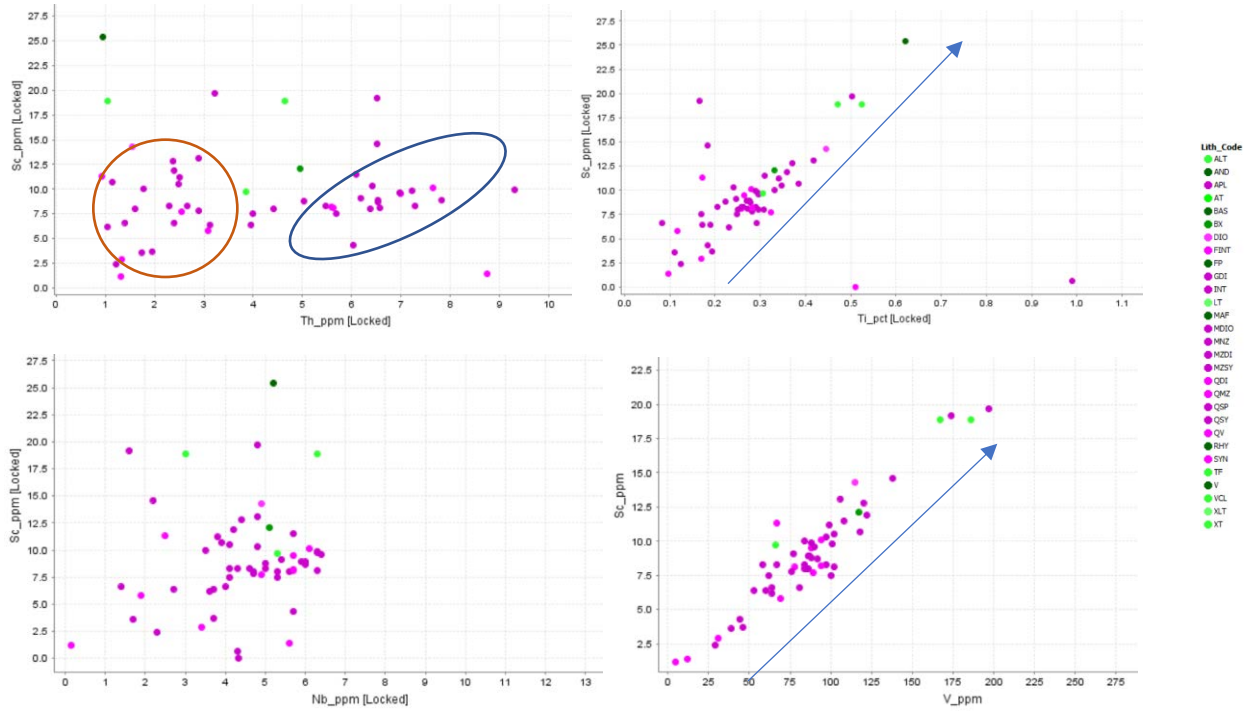


Figure 6. Sc vs Th, Ti, Nb, V show possibly two separate magmatic events.

### Al vs Ti, Sc

Most magmatic rocks contain between 6 and 9 weight percent aluminum. Low Al values are usually the result of dilution caused by hydrothermal processes. In rocks that are heavily brecciated or veined the infilling mineral dilutes the trace elements, and the immobile element plots will trend towards the origin (Barrett and MacLean 1999). So low Al percent and lower Sc will point toward potential hydrothermal processes.

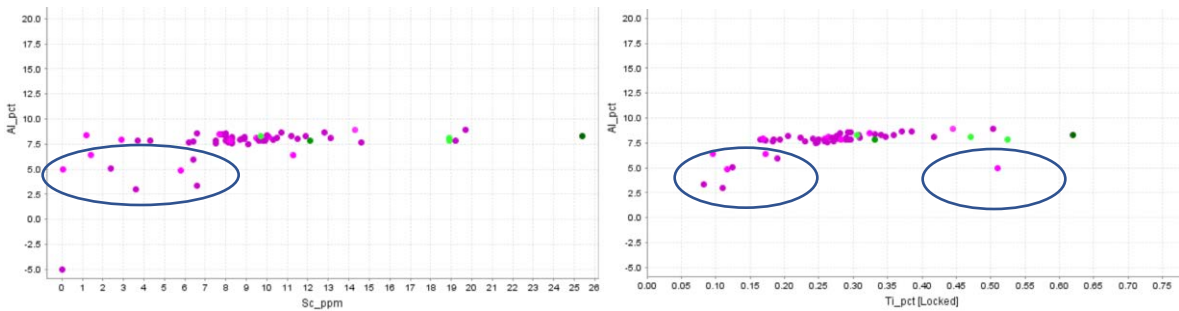


Figure 7. Al vs Ti, Sc. Evidence of hydrothermal processes

### V/Sc vs Sc

Declining V/Sc with decreasing Sc is interpreted to reflect fractional crystallization of magnetite and is a signature in magnetite-series melts (lower black arrow), none here. Increasing V/Sc with decreasing Sc is a signature of Hbl/Cpx fractionation, and prospective for Porphyry Copper (red circle) (Halley 2020).

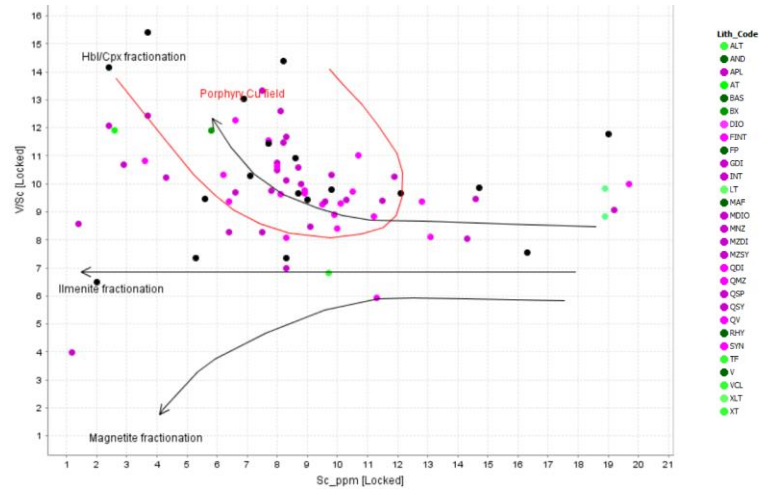


Figure 8. V/Sc vs Sc. Porphyry Cu Potential (Red Circle).

When plotted spatially the rocks located within the prospective porphyry Cu (red points) circle are located:

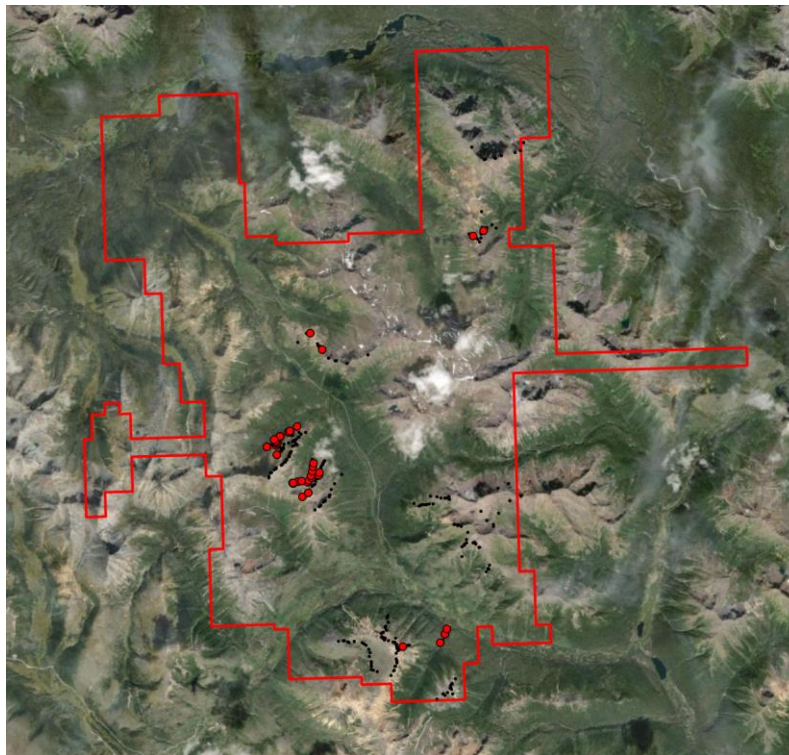


Figure 9. Map showing V/Sc vs Sc plot Porphyry Potential Hand Samples.



## Sr/Y vs Y

High Sr/Y values and low total Y is a signature observed in porphyry Cu magmas (Richards and Kerrich 2007). This plot shows magmas with high water content (adakite-like rocks) generated at high pressure (Richards 2011). Sr is mobile during hydrothermal alteration so Sr/Y may plot below the typical “Adakite” grouping in more acidic environments, as seen below (yellow circle).

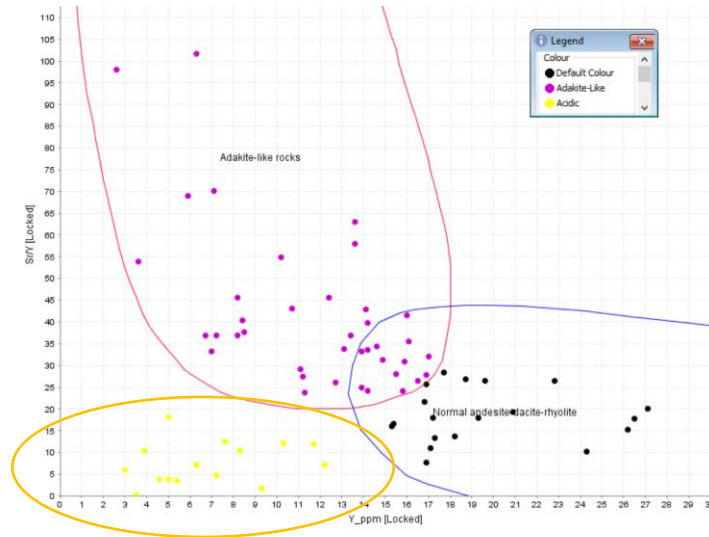


Figure 10. Adakite plot, shows magmas with higher water content.

Plotted spatially the adakite-like rocks are located (red dots: adakite like, yellow dots: plots below adakite zone, possibly acidic).

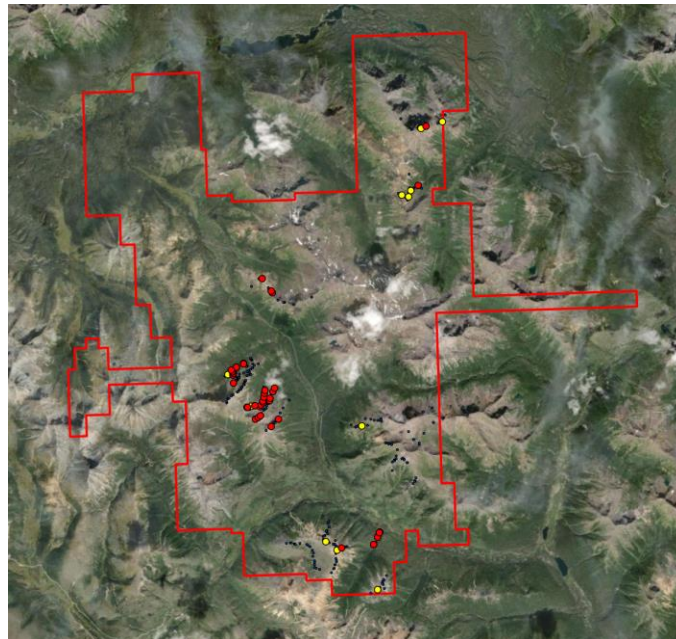


Figure 11. Map of Adakite Zone rock locations.

### Sc vs Ni, Cu

In unaltered rocks Cu is highly correlated with Sc with a ratio of about 2.5:1. In igneous rocks that do not contain olvine or clinopyroxene Ni is highly correlated with Sc at a ratio of above 1.5:1. Melts that become sulphide saturated typically show depletion of Cu and Ni, while Zn and Mn are not depleted (Halley 2020). The samples circled in blue are likely sulphide saturated.

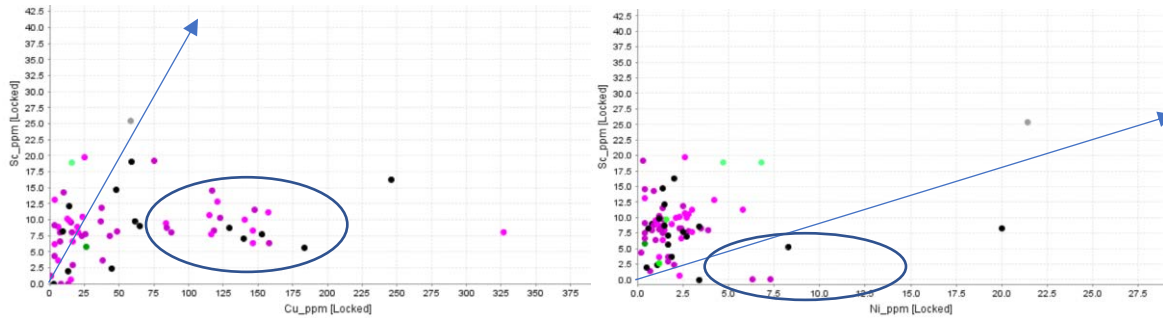


Figure 12. Sc vs Cu and Ni.

### Hf vs Zr

Hf resides primarily zircon where it substitutes for Zr (Claiborne et al 2006). Felsic magmas that are related to hydrothermal alteration typically have low Zr and a higher Hf/Zr ratio (blue line). There is a weak high Hf/Zr ratio trend below, however caution must be used due to the difficulty of dissolving zircons in a 4 acid digestion. Blue arrow = Hf/Zr of 1:20, orange arrow = Hf/Zr of 1:36.

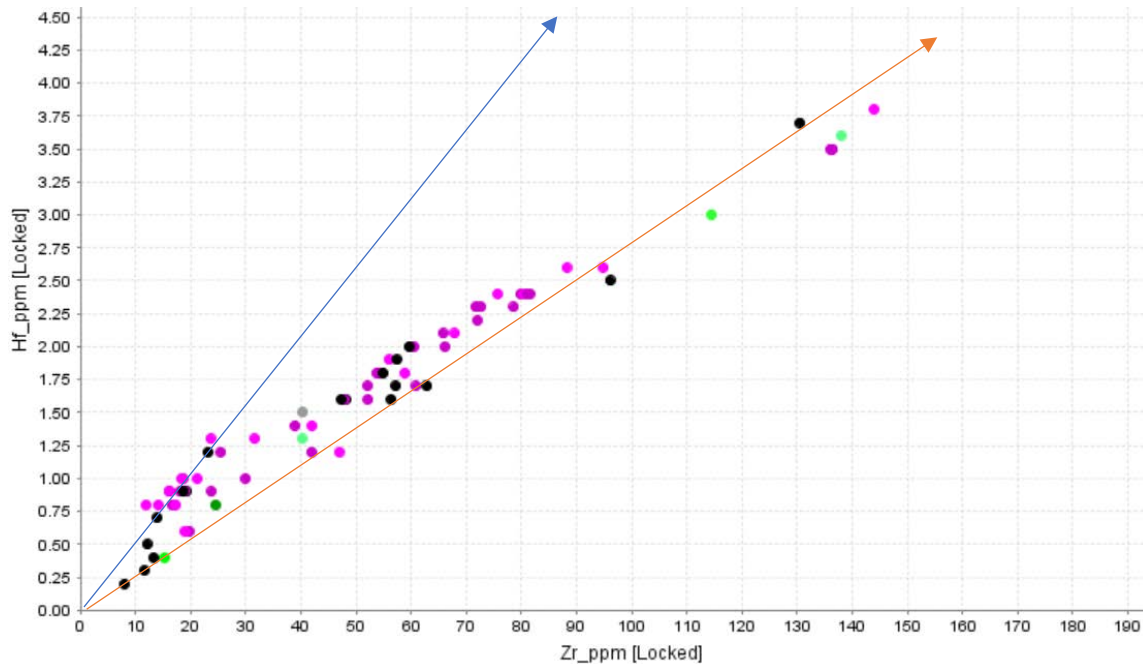


Figure 13. Hf/Zr ratio showing distinct trends.

## Ti vs Nb

Ti and Nb are often highly correlated but the way in which Ti/Nb ratios changes with fractionation depends on which mineral phase is the main repository for Ti. With fractional crystallization of magnetite the Ti content of the magma may fall to around 0.1% (which is what we see below) but Nb contents remain the same. Typical porphyry copper deposit magmas typically have between 0.2 to 0.4% Ti and 2 to 4ppm Nb, and show limited evolution with fractionation (Halley 2020).

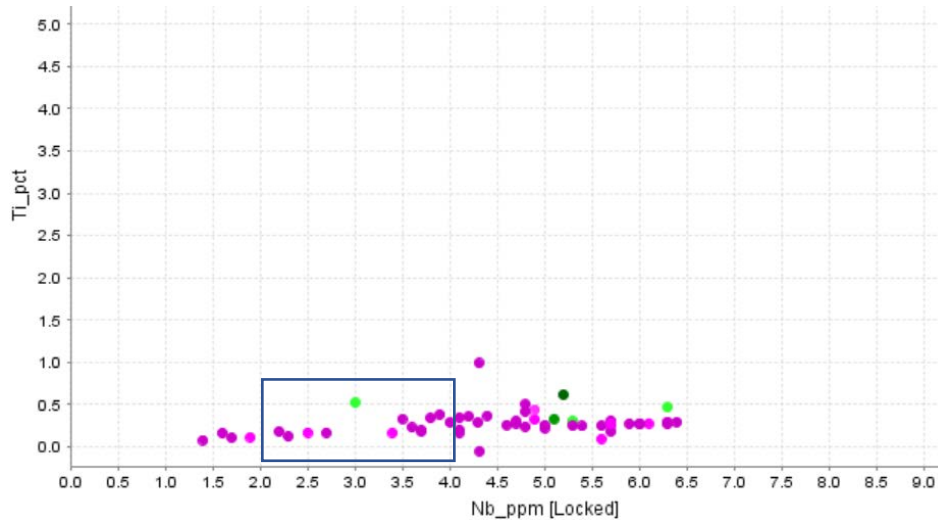


Figure 14. Ti vs Nb, magma fertility.

When plotted spatially the Nb of 2-4 ppm zone rocks (red points) are located:

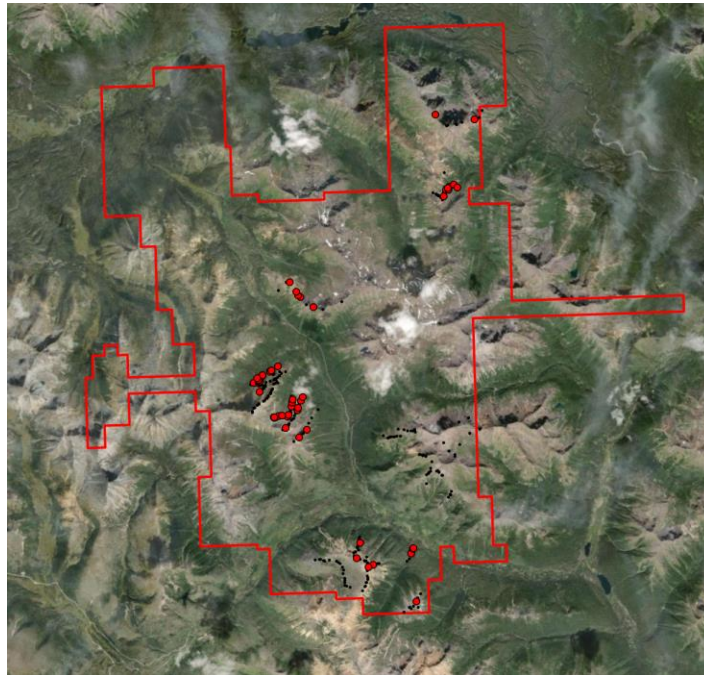


Figure 15. Ti vs Nb, porphyry zone samples plotted.

### 5.3 ALTERATION MINERALOGY

#### K/Al vs Na/Al

Most fresh magmatic rock compositions will plot between 0.3 and 0.5 Na/Al and 0.1 to 0.4 K/Al, forming a trend from mafic at low Na/Al and K/Al to felsic at higher Na/Al and K/Al. For a rock that is completely sericitized the mineralogy of the rock will be muscovite-quartz-carbonate-pyrite, resulting in all of the K and Al of the rock being within sericite zone and at a ratio of 1:3. A rock that is totally K-feldspar altered will have a K/Al ratio of 1:1 and will plot on a trajectory toward K/Al = 1 and Na/Al = 0. Albite will plot at a Na/Al of 1:1 and K/Al of 0. Kaolinite will plot at K/Al of 0 and Na/Al of 0 (Stanley and Madeisky 1996). This diagram helps separate out K-feldspar (pink), sericite (yellow), smectite (blue), and albitic (green).

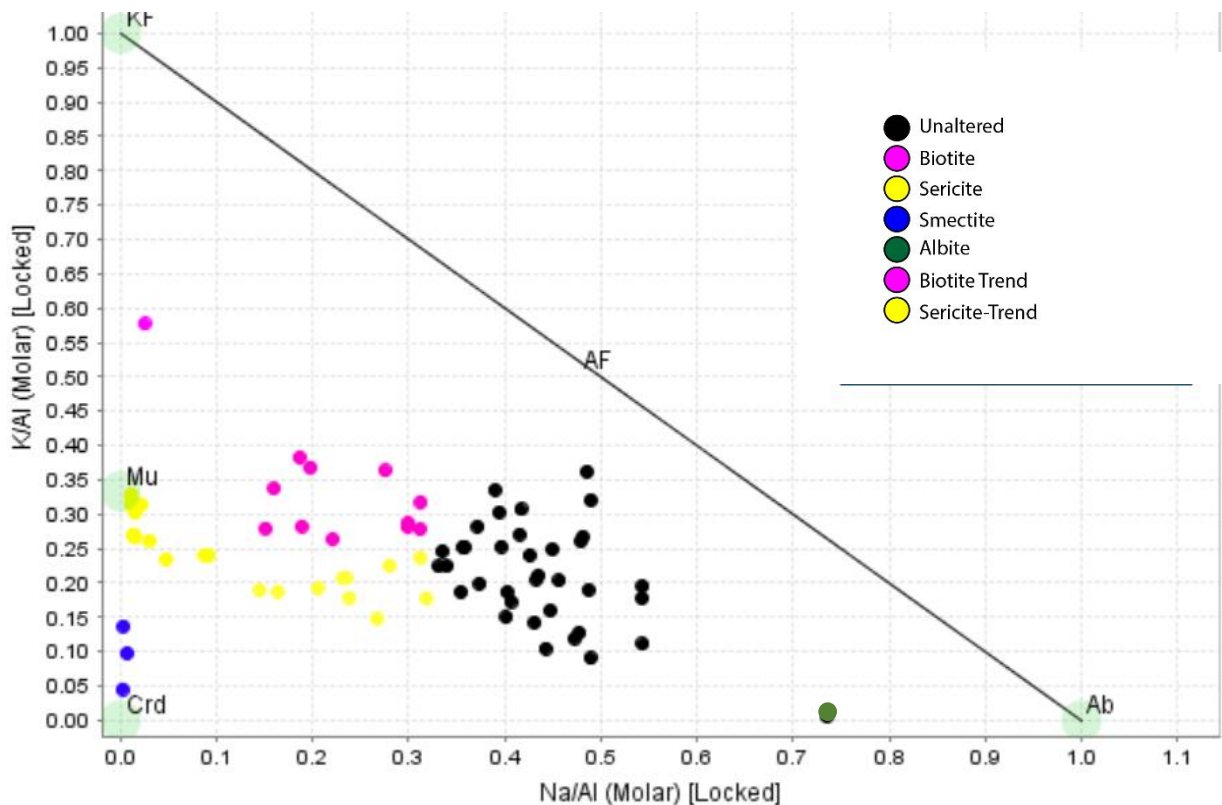


Figure 16. Feldspar GER Diagram.

When plotted spatially they show up as (pink: biotite, yellow: illite, blue: smectite):

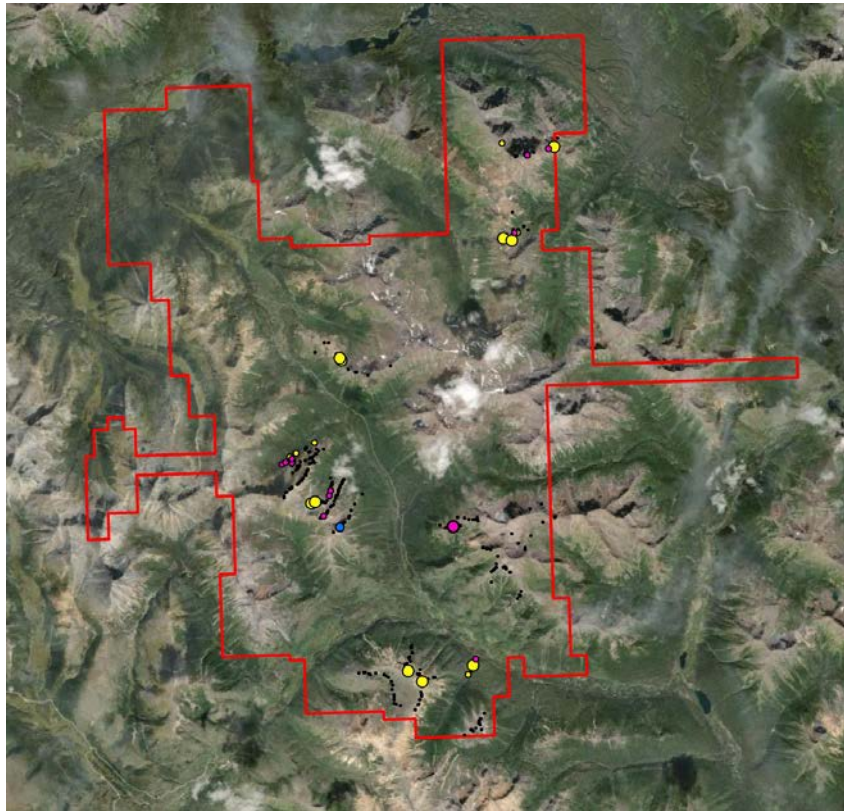


Figure 17. Location of Feldspar GER Diagram Picks.

### Al-K-Mg Ternary

The Al-K-Mg ternary plot can show physical mixtures of kaolinite, muscovite, chlorite, and potassium feldspar (Halley 2020). Here we can see all of samples are located within the muscovite (possible phyllic) and advanced argillic zones.

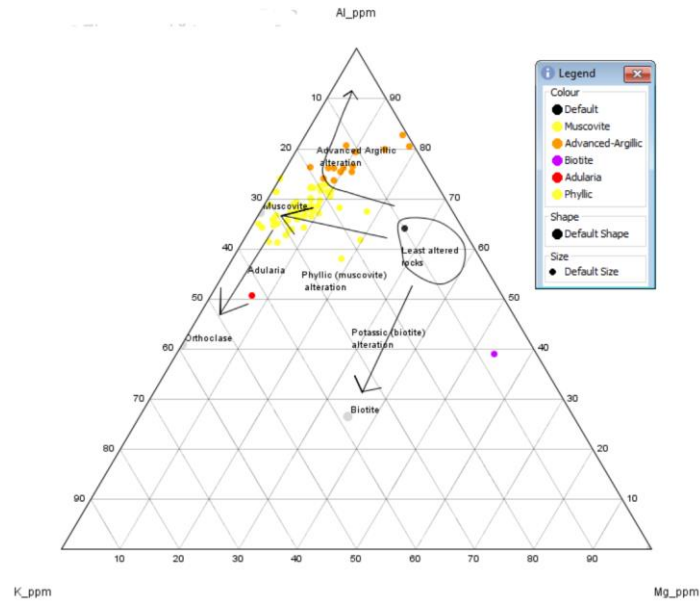


Figure 18. Al-K-Mg Ternary Diagram\

When plotted spatially:

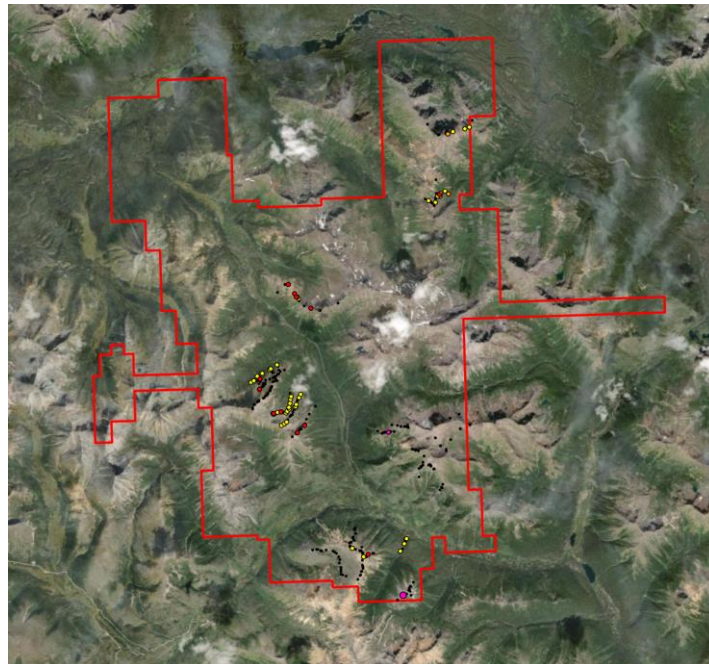


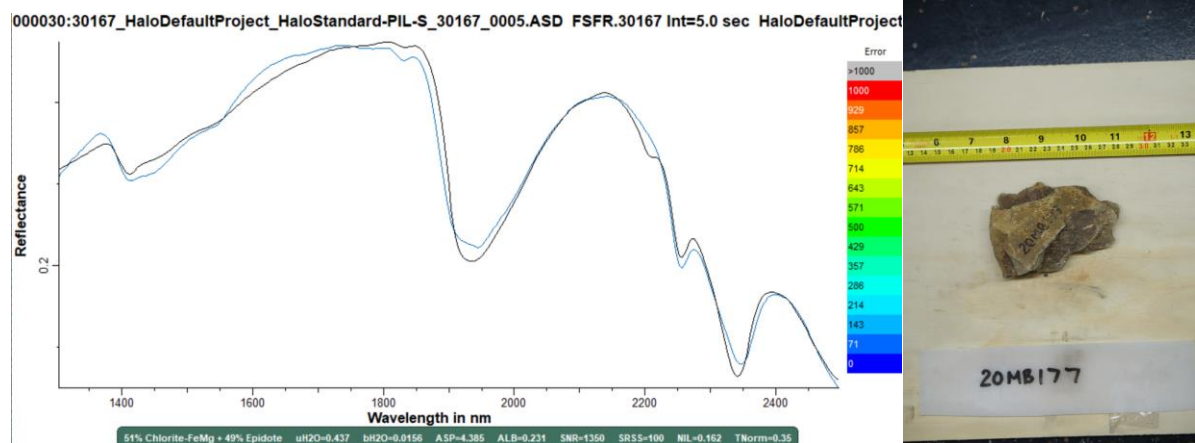
Figure 19. Spatial plot of K-Al-Mg zones

## 6 TERRASPEC ASD SWIR

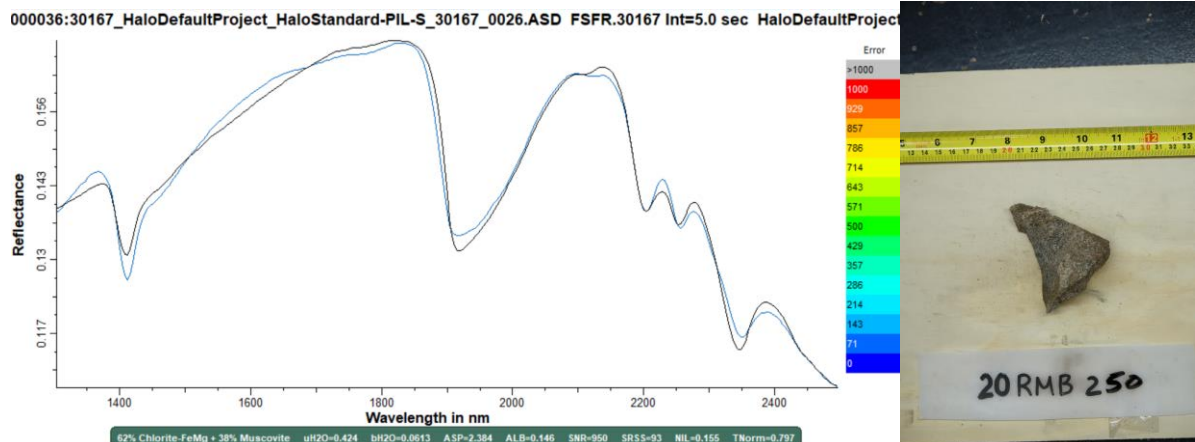
The SWIR data was collected using a handheld Terraspec Halo and processed using TSG. The Terraspec shines a light on the specimen and records the reflectance spectra over wavelengths between 1400 – 2600nm. The TSG software then compares these spectra to known mineral mixtures to determine what the likely mineral is in the rock. The spectra is manually checked and the picks are visually confirmed using TSG, and compared to photos of the hand specimens. Once the mineral picks are confirmed the minerals are placed into alteration assemblages. For PIL they fall into the following categories:



### Chlorite-Epidote (Chlorite Dominant)

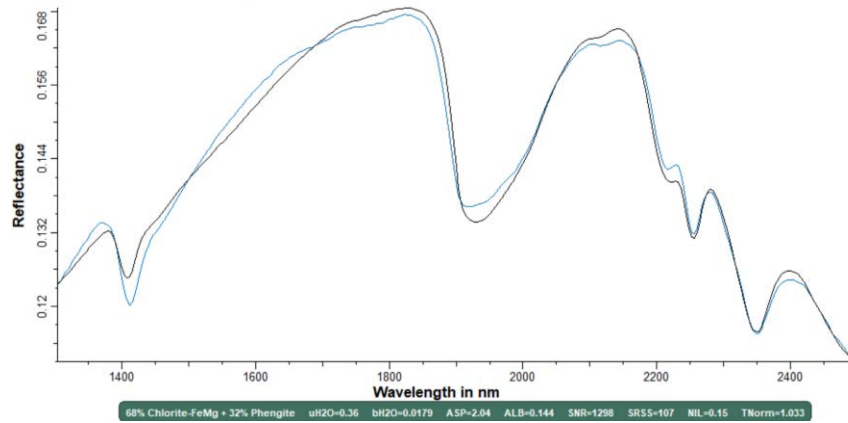


### Chlorite-Muscovite (Chlorite Dominant)



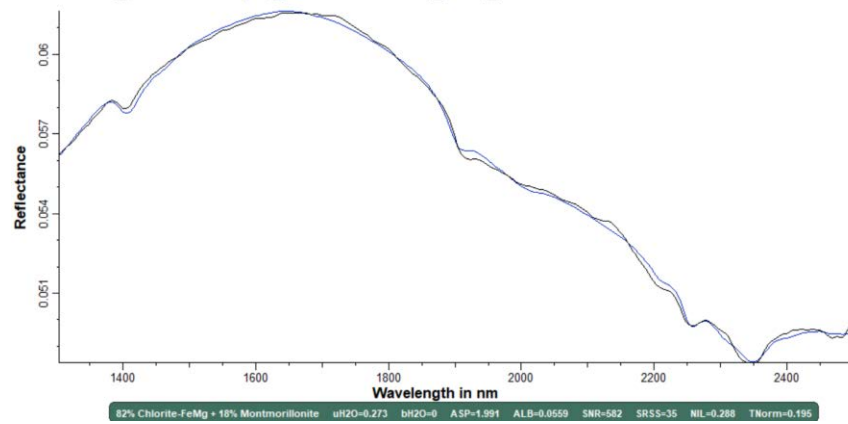
### Chlorite-Phengite (Chlorite Dominant)

000043:30167\_HaloDefaultProject\_HaloStandard-PIL-S\_30167\_0049.ASD FSFR.30167 Int=5.0 sec HaloDefaultProject



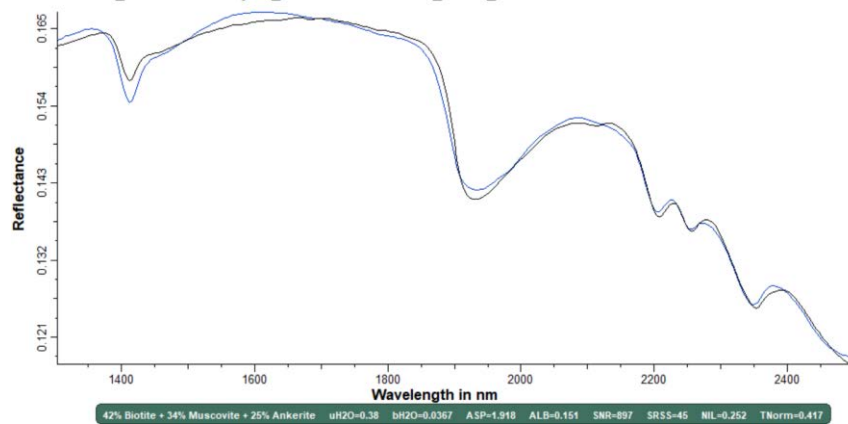
### Chlorite-Smectite (Chlorite Dominant)

000074:30167\_HaloDefaultProject\_HaloStandard-PIL-S\_30167\_0155.ASD FSFR.30167 Int=5.0 sec HaloDefaultProject



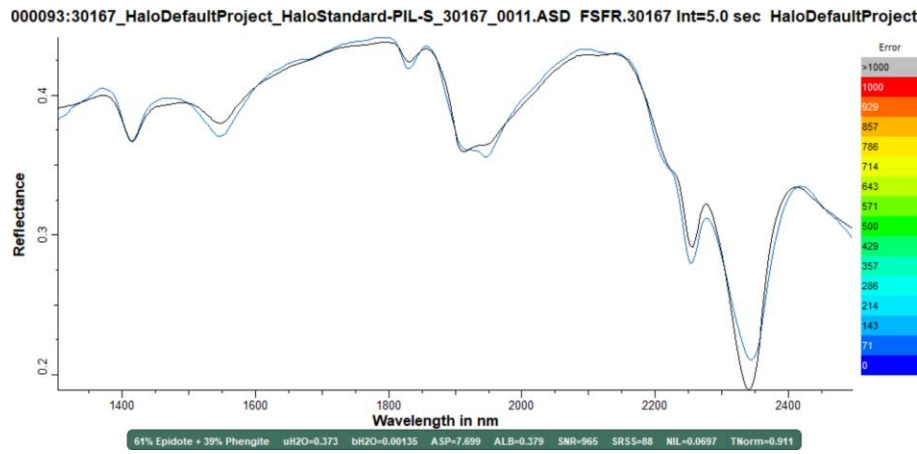
### Biotite

000027:30167\_HaloDefaultProject\_HaloStandard-PIL-S\_30167\_0205.ASD FSFR.30167 Int=5.0 sec HaloDefaultProject

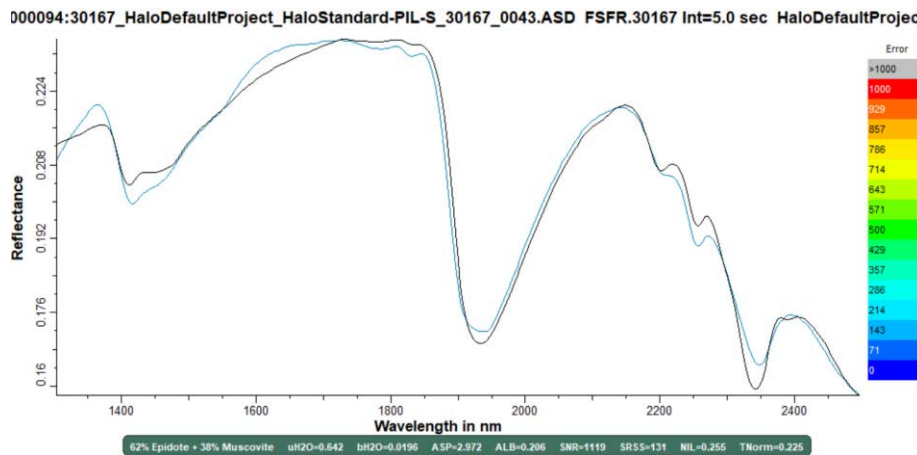




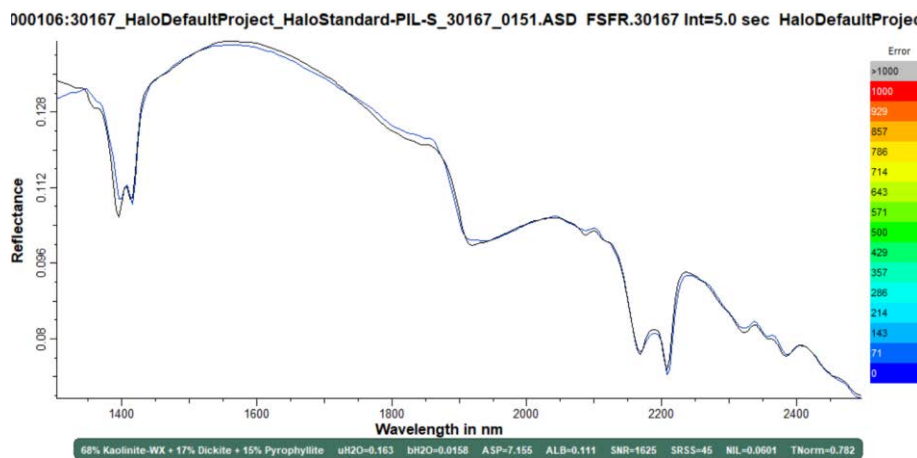
### Epidote-Phengite (Epidote Dominant)



### Epidote-Muscovite (Epidote Dominant)

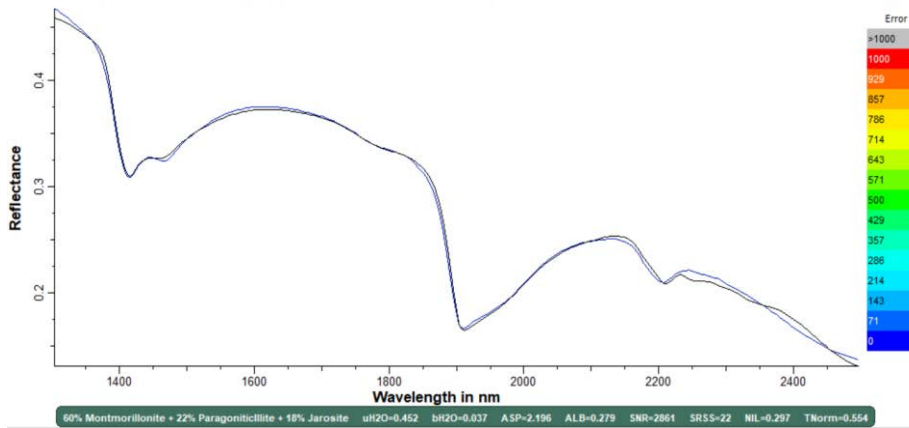


### Kaolinite-Dickite



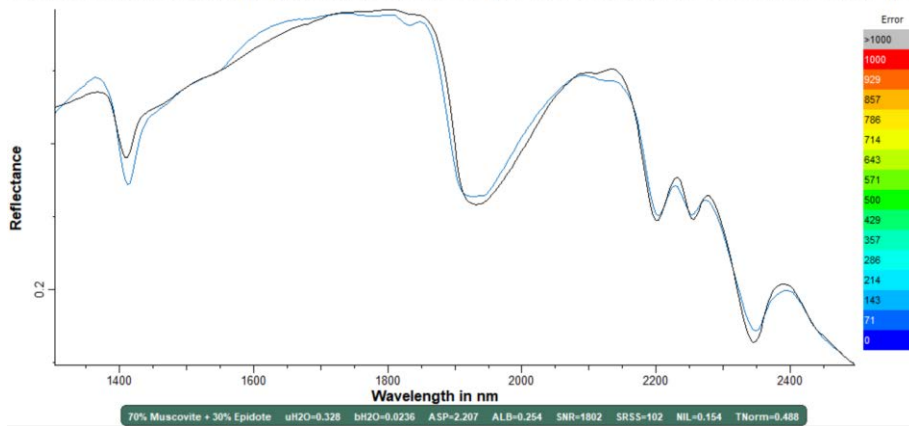
### Smectite-Illite (Smectite Dominant)

000107:30167\_HaloDefaultProject\_HaloStandard-PIL-S\_30167\_0157.ASD FSFR.30167 Int=5.0 sec HaloDefaultProject



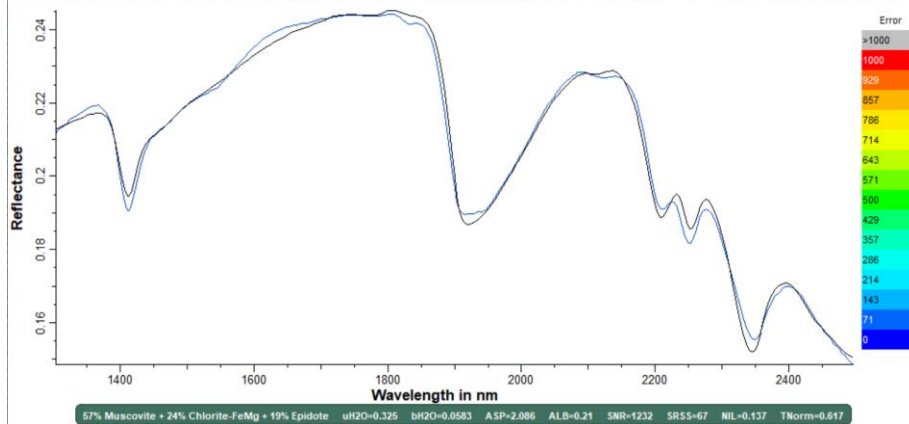
### Muscovite-Epidote (Muscovite Dominant)

000110:30167\_HaloDefaultProject\_HaloStandard-PIL-S\_30167\_0014.ASD FSFR.30167 Int=5.0 sec HaloDefaultProject



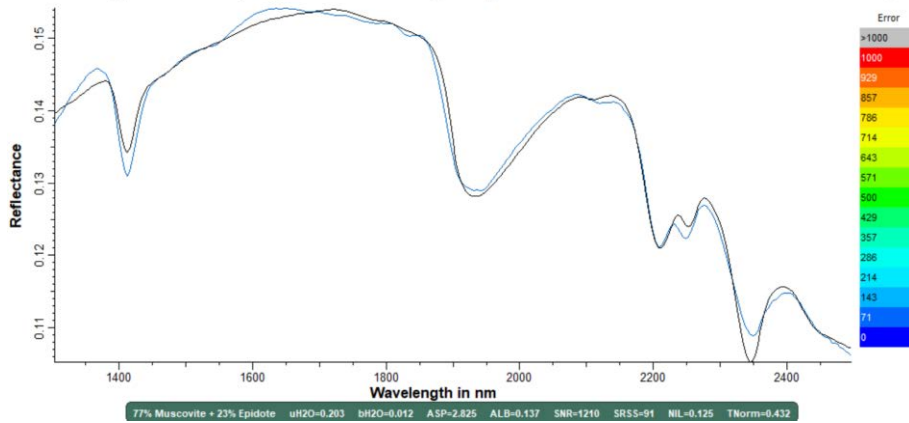
### Muscovite-Chlorite (Muscovite Dominant)

000115:30167\_HaloDefaultProject\_HaloStandard-PIL-S\_30167\_0033.ASD FSFR.30167 Int=5.0 sec HaloDefaultProject



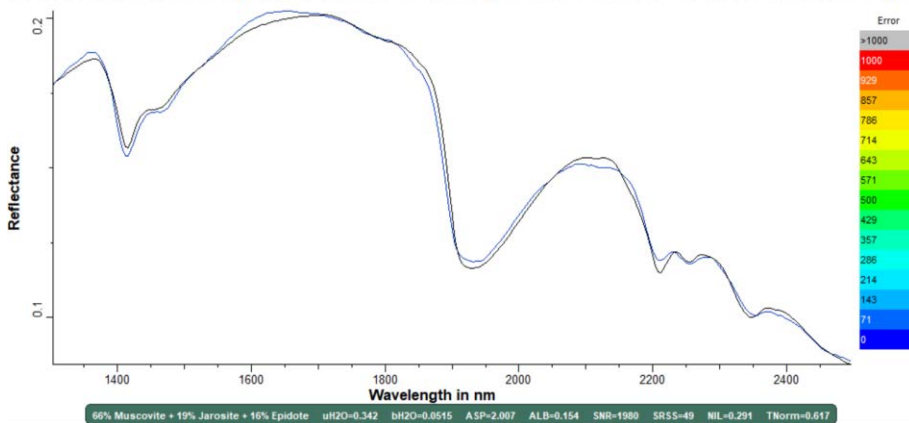
### Muscovite-Epidote (Muscovite Dominant)

000122:30167\_HaloDefaultProject\_HaloStandard-PIL-S\_30167\_0051.ASD FSFR.30167 Int=5.0 sec HaloDefaultProject



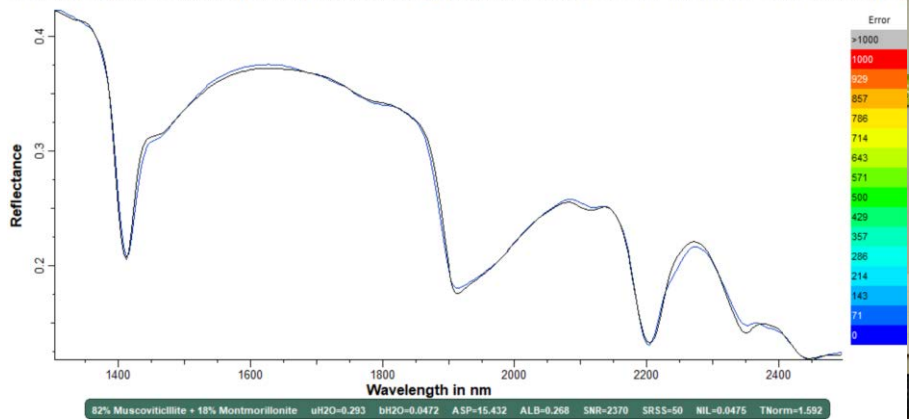
### Muscovite-Jarosite

000130:30167\_HaloDefaultProject\_HaloStandard-PIL-S\_30167\_0074.ASD FSFR.30167 Int=5.0 sec HaloDefaultProject



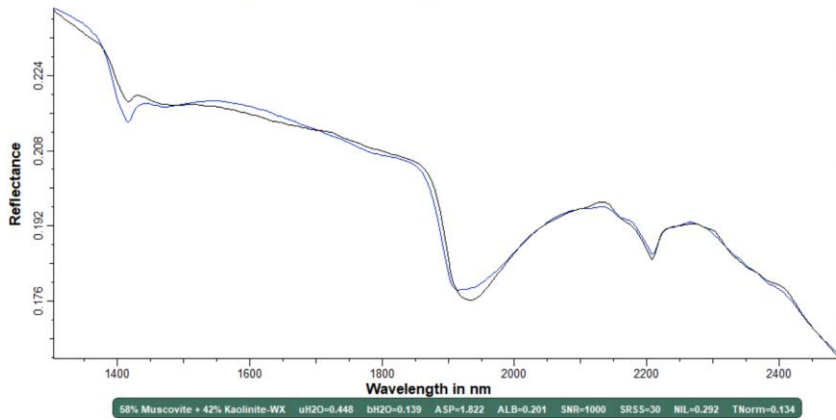
### Illite-Smectite (Illite Dominant)

000177:30167\_HaloDefaultProject\_HaloStandard-PIL-S\_30167\_0147.ASD FSFR.30167 Int=5.0 sec HaloDefaultProject



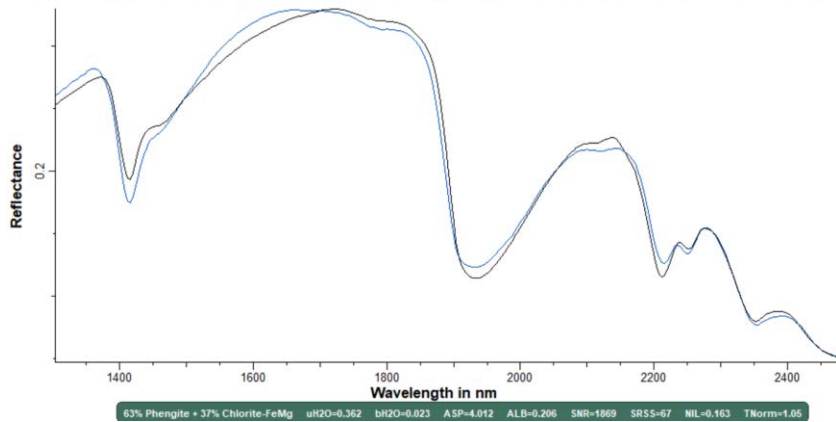
### Muscovite-Kaolinite (Muscovite Dominant)

000159:30167\_HaloDefaultProject\_HaloStandard-PIL-S\_30167\_0179.ASD FSFR.30167 Int=5.0 sec HaloDefaultProject



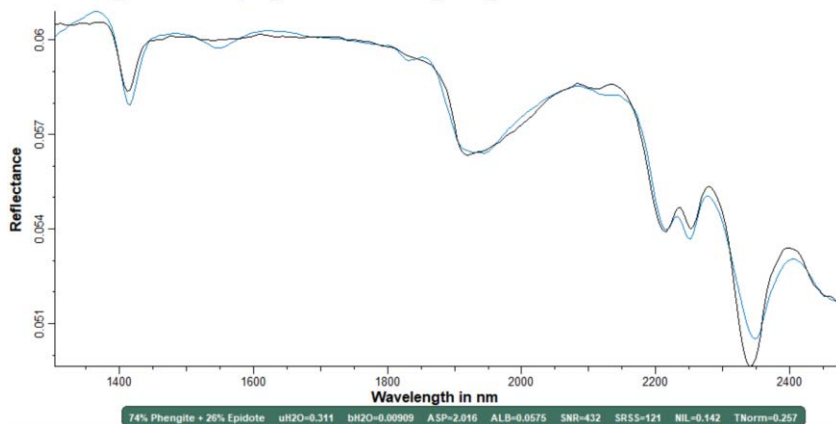
### Phengite-Chlorite (Phengite Dominant)

000185:30167\_HaloDefaultProject\_HaloStandard-PIL-S\_30167\_0023.ASD FSFR.30167 Int=5.0 sec HaloDefaultProject



### Phengite-Epidote (Phengite Dominant)

000193:30167\_HaloDefaultProject\_HaloStandard-PIL-S\_30167\_0096.ASD FSFR.30167 Int=5.0 sec HaloDefaultProject



## 7 CORRELATING SWIR AND GEOCHEMISTRY

Once the Terraspec data was processed and the mineral assemblage picks were chosen they were compared to the geochemistry alteration plots. By plotting the Al-K-Mg diagram you can see if the Terraspec corresponds with the geochemistry for alteration. In this case they match for the samples that have both Terraspec and Geochemistry data:

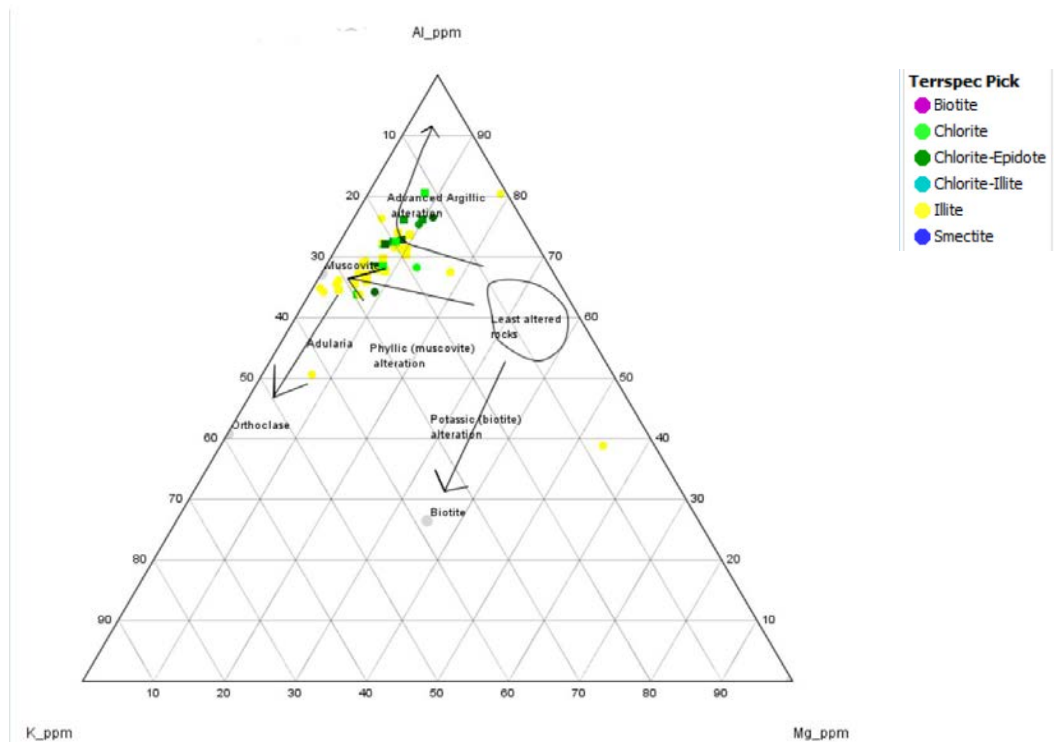


Figure 20. Terraspec picks.

## 8 TERRASPEC SPATIAL ASSOCIATIONS

Adding the location information and mapping the Terraspec mineral assemblage picks shows quite a few of the zones that were explored in 2020 sit within sericite (muscovite, illite, phengite) alteration zones. These associations make sense since the gossanous zones were targeted. Along the boundaries of the sericite zones are the chlorite and smectite dominant zones (more chlorite than illite or smectite); these areas still contain sericite, however as a secondary mineral. There is some biotite but it is difficult to say if it is primary or secondary biotite. Within the sericite zone there is higher temperature muscovite, lower temperature illite, and less acidic phengite. In some places the sericite is associated with jarosite. Within the smectite zone there is higher temperature dickite, its lower temperature pseudomorph kaolinite, as well as montmorillonite. The chlorite zones include sericite when in proximity to the sericite zones, and epidote when away from the sericite zones. Epidote dominated mineralogy appears on the periphery.

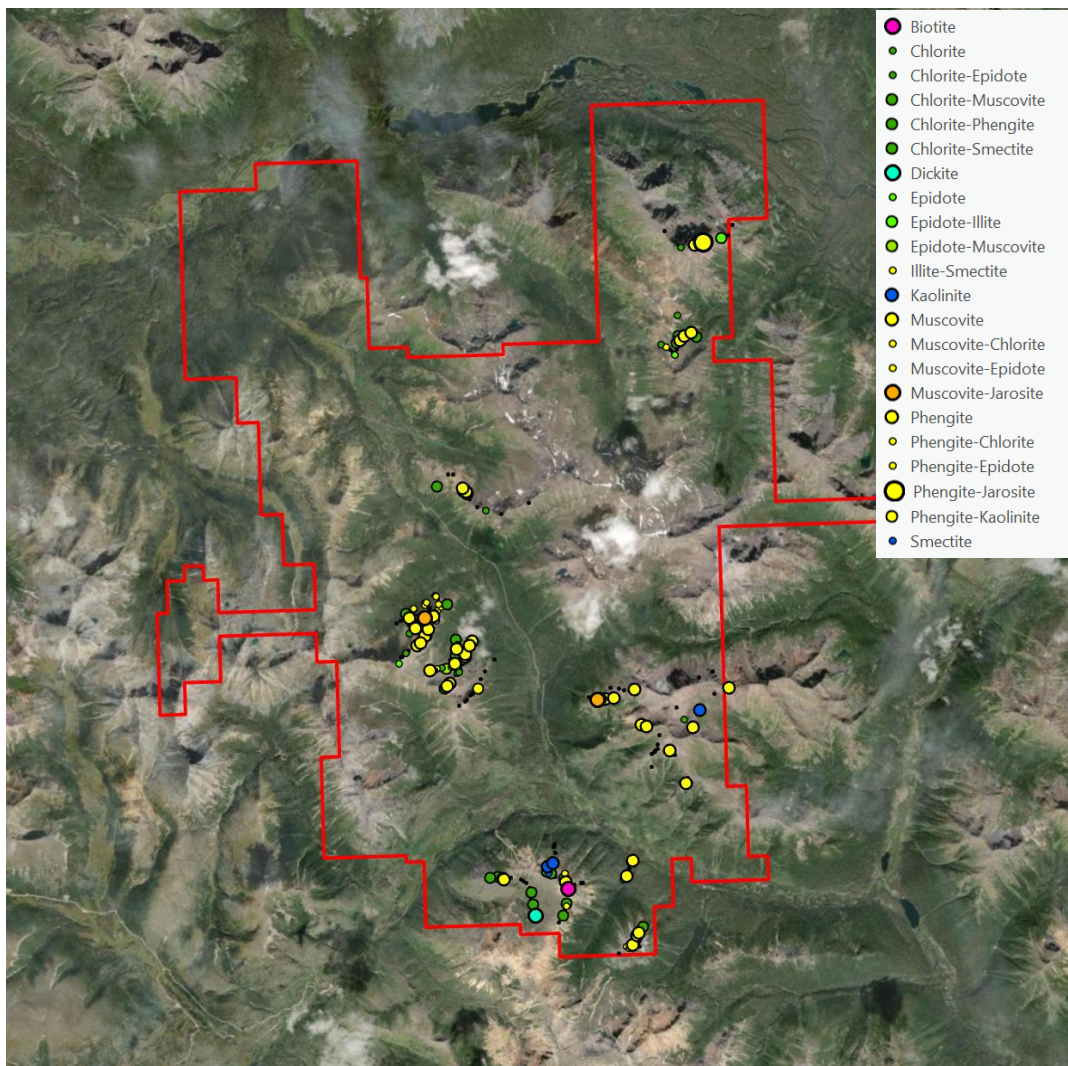


Figure 21. Terraspec data on map.

## 9 PATHFINDERS

There are various trace elements that can be used as pathfinders for porphyry systems. The vertical distribution of trace elements in rock samples show distinct variations depending on where in the system the rock is located. Near the top of an idealized system you should see elevated tellurium (Tl) and lithium (Li). Further down elevated bismuth (Bi) and arsenic (As) grading into elevated tungsten (W) and molybdenum (Mo), then finally elevated copper (Cu).

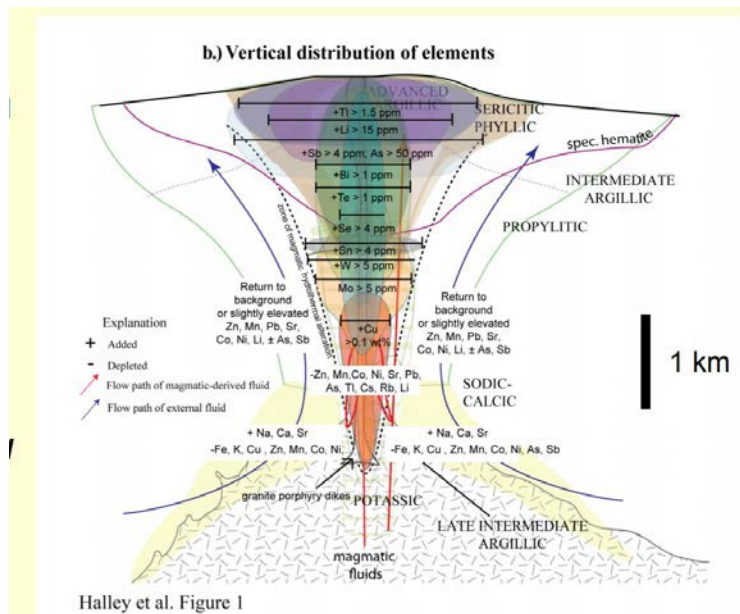
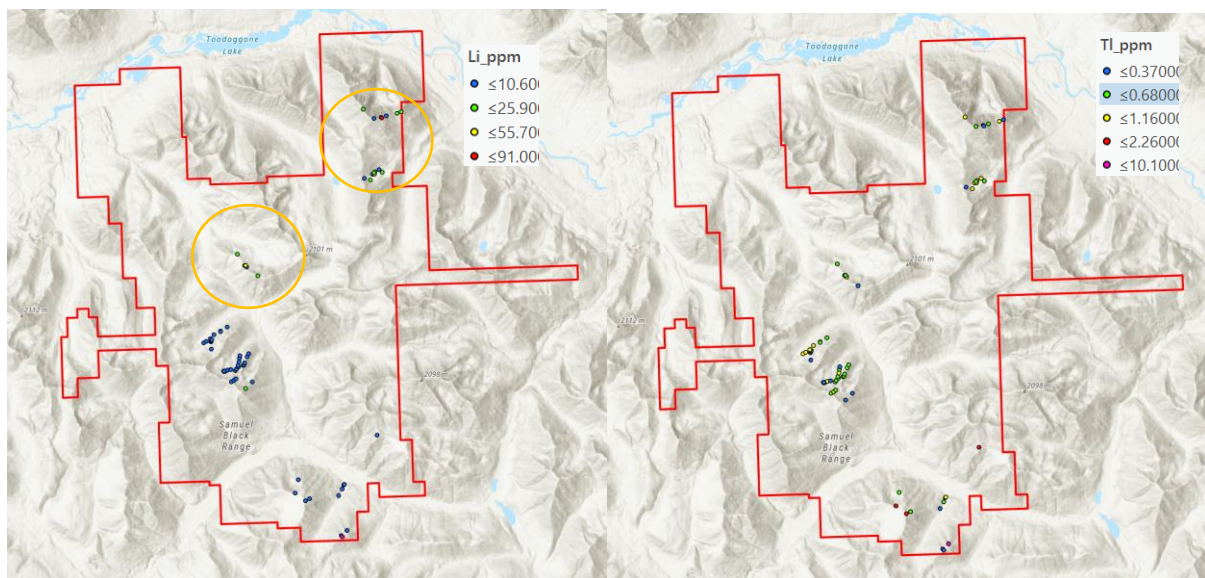
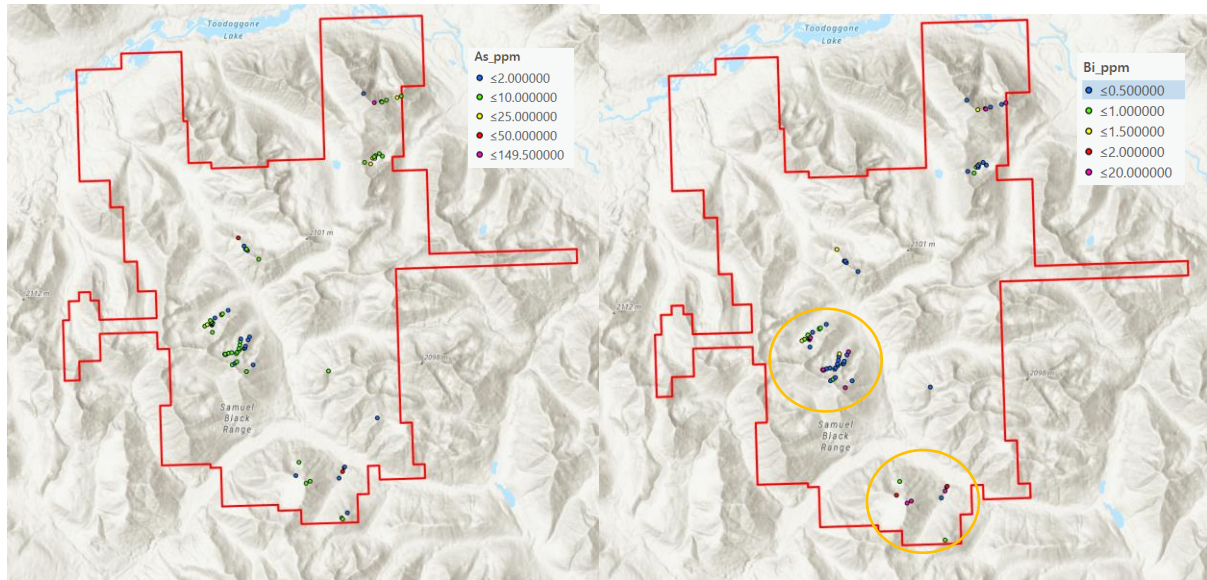


Figure 22. Pathfinder elements over an idealized porphyry model. Tosal and Halley 2011.

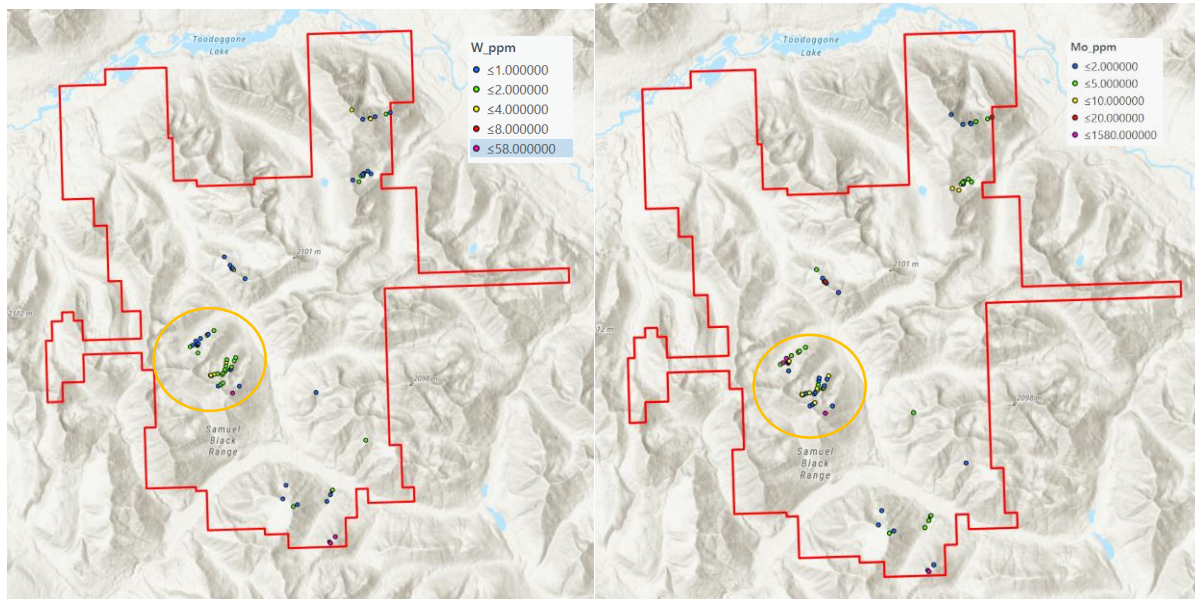
There is elevated (greater than 1.5ppm) Tl in every zone visited in 2020. Lithium is elevated over the northern targets (NE, North). This shows that those zones are potentially argillic on surface.



There is elevated Arsenic and Bismuth over the southern targets (Central, Copper Ridge, and PIL South), meaning that the alteration may be from deeper in the system:

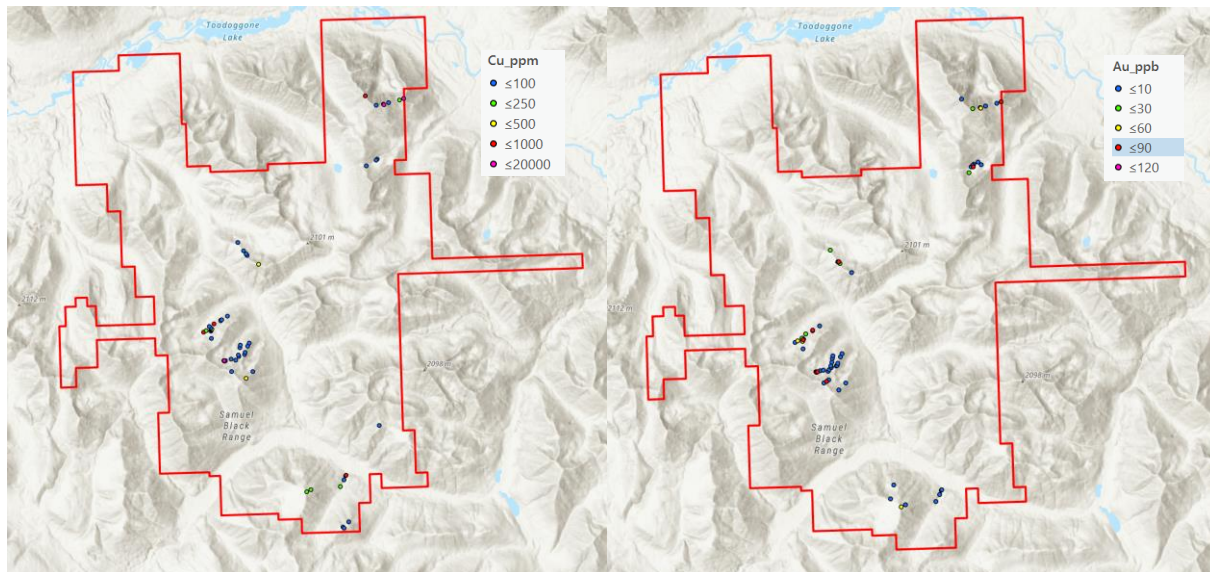


Tungsten and Molybdenum are elevated in samples over the central target, meaning that these zones could possibly be nearer the heat and fluid source:





Copper and Gold values are spotty over all the areas targeted, which shows that the current elevation has not fully cut into any large potassic zones (likely buried), or could be epithermal veins.



## 10 SUMMARY

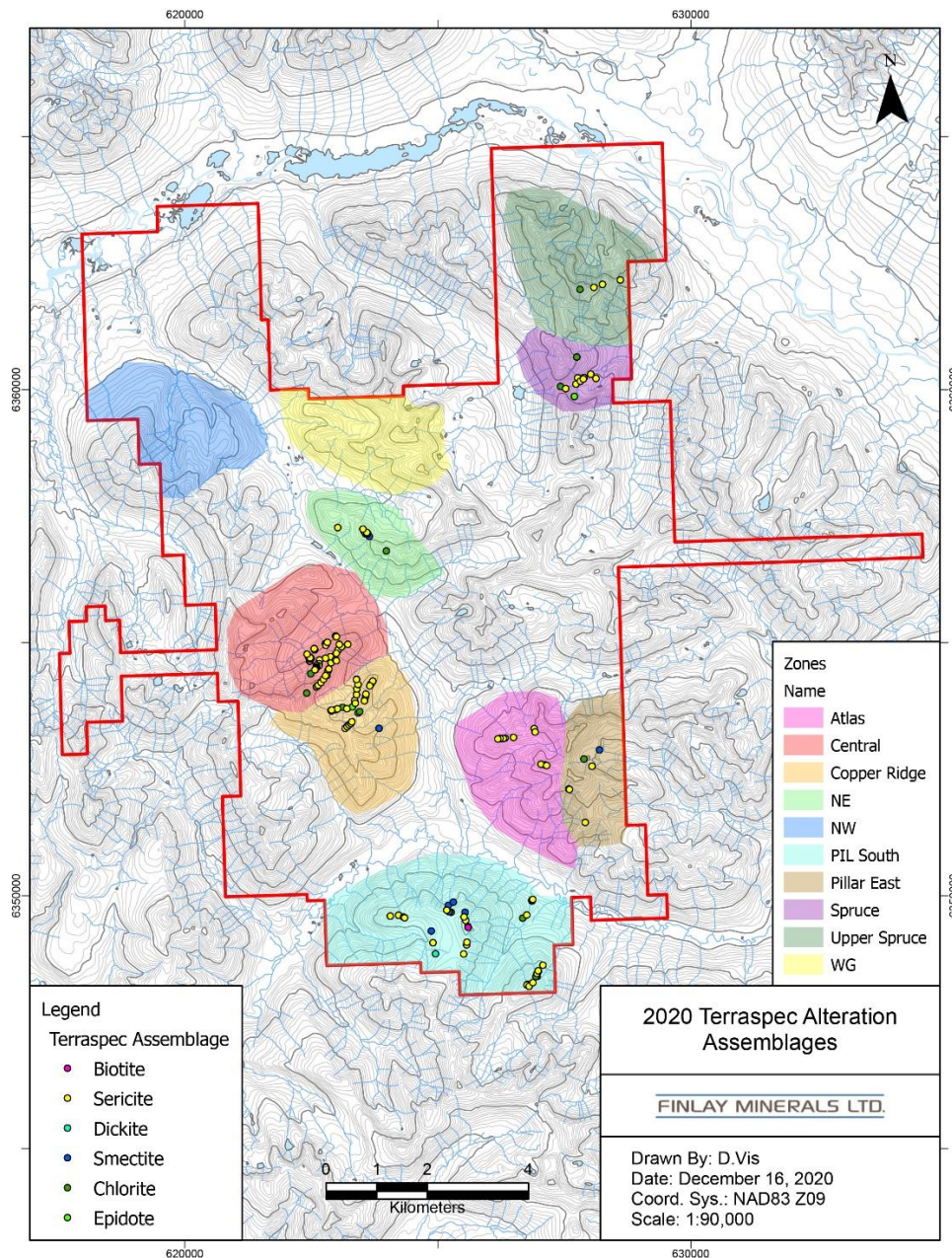
From the geochemistry we can see that there are zones of metal enrichment and there was likely at least two magmatic events (multiphase intrusives). As for porphyry magma potential several of the samples show high V/Sc, low Sc zones that could correlate to Hbl/Cpx fractionation, which can be an indicator for hydrothermal magmatic processes. Several of the samples also plot within or just below the adakite zone showing a wet magma, which is key for developing hydrothermal magmatic systems. Some of the melts plot within the Ti/Nb zone favorable for porphyry systems (2-6ppm Nb), however the Titanium is low. In summary many of the intrusives sampled have the right stuff to be fertile porphyry magmas.

From the alteration plots there is various hydrothermal alteration zones present, biotite/Kspar (possibly potassic), illite (largely the more basic phengite), and smectite (possibly argillic with higher temperature dickite).

The Terraspec data supports the geochemistry showing several alteration assemblages including biotite, sericite, chlorite-sericite, chlorite-epidote, chlorite-smectite, and smectite. These assemblage picks correlate with the alteration geochemistry, and from visual alteration seen in hand samples. Within the respective alteration zones various high temperature alteration minerals were picked out including dickite and muscovite, as well as the more basic phengite within the sericite zone.

The pathfinders correlate with the Terraspec and geochemistry in showing that there are a number of alteration zones with varying compositions over the property. The hottest alteration is likely located within the Central/Copper Ridge Zone and shows largely sericite style alteration

with higher temperature pathfinders. The Spruce Zone is likely higher up in the system and could be argillic. The PIL South Zone holds potential but seems constrained on surface. Atlas and Pillar East Zones need further review with more data.



In summary the PIL Property hosts fertile magmas and favorable alteration that is often associated with a hydrothermal magmatic system. Caution should always be used when interpreting trace geochemistry however by using several different element ratios, Terraspec analysis, and visual identification in hand sample, we have numerous corroborating sources of evidence to support these findings. Further work is needed to determine the full extent of the anomalies, as well as the style of mineralization, be it porphyry, epithermal, or both.

## 11 RECOMMENDATIONS

---

The historic data should be processed for geochemistry including alteration, magma fertility, and pathfinders using the 2020 data as a reference. Further Terraspec sampling should be completed across the alteration zones, preferably with a narrow, standard spacing to aid in vectoring towards hotter parts of the system.

## 12 REFERENCES

---

- Claiborne, L.L., Miller, C.F., Walker, B.A., Wooden, J.L., Mazdab, F.K., and Bea, F., 2006. Tracking Magmatic Processes through Zr/Hf Ratios in Rocks and Hf and Ti zoning in Zircons: An example from the Spirit Mountain Batholith, Nevada: *Mineralogical Magazine*, v. 70, no. 5, p. 517–543.
- Barrett, T.J., and MacLean, W.H., 1999. Volcanic sequences, lithochemistry, and hydrothermal alteration in some bimodal volcanic massive sulfide systems: *Reviews in Economic Geology*, v. 8, p. 101–131.
- Gruenwald, W., 2018. Trenching and Geological Assessment Report on the PIL Property: Assessment Report 37781.
- Halley, Scott, 2020. Mapping Magmatic and Hydrothermal Processes from Routine Exploration Geochemical Analysis: *Economic Geology*.
- Richards, J.P., 2011. High Sr/Y Arc Magmas and Porphyry Cu ± Mo ± Au Deposits: Just Add Water: *Economic Geology*, v. 106, no. 7, p. 1075–1081.
- Richards, J.P., and Kerrich, R., 2007. Special paper: Adakite-like rocks: Their diverse origins and questionable role in metallogenesis: *Economic Geology*, v. 102, no. 4, p. 537–576.
- Stanley, C.R., and Madeisky, H.E., 1996. Lithochemical Exploration for Metasomatic Zones associated with Hydrothermal Mineral Deposits using Pearce Element Ratio Analysis: British Columbia, Canada, Mineral Deposit Research Unit, Short Course Notes on Pearce Element Ratio Analysis, p. 99.
- Tosdal, R.M., Halley, S.W., 2011. Porphyry 101 A Practical Guide to Porphyry Cu (-Mo-Au) Deposits. Short Course, Perth Australia Sept. 21, 2011.
- Wilkinson, J.J., Chang, Z., Cooke, D.R., Baker, M.J., Wilkinson, C.C., Inglis, S., Chen, H., and Gemell, J.B., 2015. The Chlorite Proximitator: A New Tool for Detecting Porphyry Ore Deposits: *Journal of Geochemical Exploration*, v. 152, p. 10–26.
- Williams-Jones, A.E., and Vasyukova, O.V., 2018. The Economic Geology of Scandium, the Runt of the Rare earth Element Litter: *Economic Geology*, v. 113, no. 4, p. 973–988.